

White matter hyperintensity patterns in cerebral amyloid angiopathy and hypertensive arteriopathy



Andreas Charidimou, MD, PhD
Gregoire Boulouis, MD
Kellen Haley, BSc
Eitan Auriel, MD
Ellis S. van Etten, MD
Panagiotis Fotiadis
Yael Reijmer, PhD
Alison Ayres, BA
Anastasia Vashkevich, BA
Zora Y. Dipucchio, BA
Kristin M. Schwab, BA
Sergi Martinez-Ramirez
Jonathan Rosand, MD, MSc
Anand Viswanathan, MD, PhD
Steven M. Greenberg, MD, PhD
M. Edip Gurol, MD, MSc

Correspondence to
Dr. Gurol:
edip@mail.harvard.edu

ABSTRACT

Objective: To identify different white matter hyperintensity (WMH) patterns between 2 hemorrhage-prone cerebral small vessel diseases (SVD): cerebral amyloid angiopathy (CAA) and hypertensive arteriopathy (HA).

Methods: Consecutive patients with SVD-related intracerebral hemorrhage (ICH) from a single-center prospective cohort were analyzed. Four predefined subcortical WMH patterns were compared between the CAA and HA groups. These WMH patterns were (1) multiple subcortical spots; (2) peri-basal ganglia (BG); (3) large posterior subcortical patches; and (4) anterior subcortical patches. Their associations with other imaging (cerebral microbleeds [CMBs], enlarged perivascular spaces [EPVS]) and clinical markers of SVD were investigated using multivariable logistic regression.

Results: The cohort included 319 patients with CAA and 137 patients with HA. Multiple subcortical spots prevalence was higher in the CAA compared to the HA group (29.8% vs 16.8%; $p = 0.004$). Peri-BG WMH pattern was more common in the HA- vs the CAA-ICH group (19% vs 7.8%; $p = 0.001$). In multivariable logistic regression, presence of multiple subcortical spots was associated with lobar CMBs (odds ratio [OR] 1.23; 95% confidence interval [CI] 1.01–1.50, $p = 0.039$) and high degree of centrum semiovale EPVS (OR 2.43; 95% CI 1.56–3.80, $p < 0.0001$). By contrast, age (OR 1.05; 95% CI 1.02–1.09, $p = 0.002$), deep CMBs (OR 2.46; 95% CI 1.44–4.20, $p = 0.001$), total WMH volume (OR 1.02; 95% CI 1.01–1.04, $p = 0.002$), and high BG EPVS degree (OR 8.81; 95% CI 3.37–23.02, $p < 0.0001$) were predictors of peri-BG WMH pattern.

Conclusion: Different patterns of subcortical leukoaraiosis visually identified on MRI might provide insights into the dominant underlying microangiopathy type as well as mechanisms of tissue injury in patients with ICH. *Neurology*® 2016;86:505–511

GLOSSARY

BG = basal ganglia; **CAA** = cerebral amyloid angiopathy; **CI** = confidence interval; **CMB** = cerebral microbleeds; **CSO** = centrum semiovale; **EPVS** = enlarged perivascular spaces; **FLAIR** = fluid-attenuated inversion recovery; **HA** = hypertensive arteriopathy; **ICH** = intracerebral hemorrhage; **MGH** = Massachusetts General Hospital; **OR** = odds ratio; **PV** = periventricular; **SC** = subcortical; **SVD** = small vessel disease; **TE** = echo time; **VBM** = voxel-based morphometry; **WMH** = white matter hyperintensities.

Sporadic cerebral amyloid angiopathy (CAA) and hypertensive arteriopathy (HA) are the 2 most common forms of cerebral small vessel disease (SVD) in older adults.¹ CAA results from β -amyloid deposition within cortical and leptomeningeal arteries whereas HA predominantly affects small perforating end-arteries of the deep gray nuclei and deep white matter. Both CAA and HA are common causes of intracerebral hemorrhage (ICH)^{2,3} and cognitive impairment.⁴ As they have intrinsically different pathophysiology, clinical significance, and prognosis,¹ specific imaging markers are needed to better understand potential disease mechanisms and facilitate future trials.⁵

Both CAA and HA are associated with characteristic neuroimaging markers, including cerebral microbleeds (CMB),⁶ white matter hyperintensities (WMH),⁷ and enlarged perivascular

From the Hemorrhagic Stroke Research Program, Department of Neurology, Massachusetts General Hospital Stroke Research Center (A.C., G.B., K.H., E.A., E.S.v.E., P.F., Y.R., A.A., A. Vashkevich, Z.Y.D., K.M.S., S.M.-R., J.R., A. Viswanathan, S.M.G., M.E.G.), and Division of Neurocritical Care and Emergency Neurology, Massachusetts General Hospital (J.R.), Harvard Medical School, Boston, MA.

Go to Neurology.org for full disclosures. Funding information and disclosures deemed relevant by the authors, if any, are provided at the end of the article.

spaces (EPVS).^{8,9} Lobar micro/macroleeds are consistently associated with CAA whereas deep bleeds are associated with HA.⁶ There is ample evidence suggesting a causal link between vascular amyloid and WMH^{10–12} but no characteristic patterns were identified for CAA, HA, or other cohorts.^{7,13,14} Small (spots) and larger (patches) areas of strictly subcortical WMH as well as linear peri–basal ganglia (BG) hyperintensities are commonly seen in clinical and research MRI but their significance is not known.

In the present study, we sought to identify differences in WMH patterns between CAA and HA in a large prospective cohort of ICH patients. To that end, 4 predefined subcortical WMH patterns were compared between the 2 groups and independent associations with other imaging and clinical markers of SVD were investigated. We also compared the volume of subcortical and periventricular WMH between these groups.

METHODS Study population and diagnostic group

assignment. We analyzed prospectively collected data from consecutive patients admitted to Massachusetts General Hospital (MGH) with spontaneous symptomatic ICH (presumed to be due to SVD after adequate evaluation¹⁵) who had MRI and enrolled in an ongoing cohort study as described extensively in previous publications.^{16–18} Patients with strictly lobar hemorrhages (including ICH and CMBs) involving the cerebral cortex and underlying white matter were coded as CAA per Boston criteria.¹⁹ The CAA-related ICH diagnosis included (1) definite, pathologically proven CAA based on full autopsy; (2) probable CAA with supporting pathology, i.e., lobar ICH with or without lobar CMBs and pathologic evidence of CAA; (3) probable CAA, based on the presence of lobar ICH and purely lobar CMBs; and (4) possible CAA, single lobar ICH without CMB. Patients with strictly deep hemorrhages in the BG, thalamus, or brainstem were diagnosed with HA. HA might not be merely related to hypertension, but the term is historically and widely used in the field to denote a sporadic non-CAA-related small vessel process that is mainly vascular risk factor–driven.¹ This group included patients with purely deep hemorrhages, i.e., deep ICH, with or without deep CMBs, but no lobar CMBs. Patients with lower diagnostic certainty, such as participants with a mixed distribution of ICH and CMBs (i.e., a lobar ICH with deep CMB, a deep ICH with lobar CMB, or brainstem ICH and lobar CMB) ($n = 49$), as well as 27 cases with cerebellar bleeds and 11 cases with other (e.g., inflammatory CAA), were excluded from the study. All patients had CT angiography/magnetic resonance angiography and vascular malformation or other ICH etiologies were ruled out.

Clinical and APOE genotype data. Patient enrollment, clinical data collection, and MRI acquisition were performed as described previously.^{16–18} In brief, the following clinical variables were systematically recorded for each participant: age, sex, presence of hypertension, diabetes, hypercholesterolemia, history of

ICH, and antithrombotic drug use at baseline. Hypertension was defined as previous diagnosis of hypertension ($>140/90$ mm Hg) or use of antihypertensive treatment for blood pressure control. Diabetes and hypercholesterolemia were defined as previous diagnoses or current use of antidiabetic and antihyperlipidemic drugs, respectively.

DNA was extracted and *APOE* genotype was determined in a subset of patients who provided blood samples as detailed elsewhere.²⁰ DNA samples were available from 276 of the 456 study participants.

Standard protocol approvals, registrations, and patient

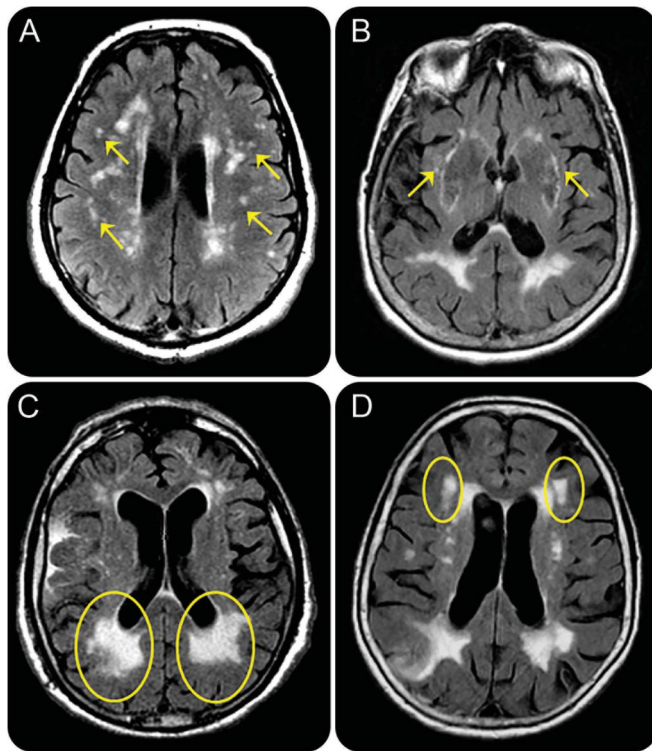
consents. This study was performed with approval and in accordance with the guidelines of the institutional review boards MGH, which allows us to collect data on all participants with ICH treated at MGH.

Neuroimaging acquisition and analysis. Images were obtained using a 1.5T MRI scanner (GE Sigma, Cleveland, OH) and included whole brain T2-weighted, T2*-weighted gradient recalled echo (echo time [TE] 750/50 ms, 5 mm slice thickness, 1 mm interslice gap), and fluid-attenuated inversion recovery (FLAIR; repetition time/TE 10,000/140 ms, inversion time 2,200 ms, 1 number of excitations, 5 mm slice thickness, 1 mm interslice gap).

Total, subcortical (SC), and periventricular (PV) WMH volumes of CAA-ICH and HA-related ICH were quantitatively measured on FLAIR MRI, in the ICH-free hemisphere, using a 2-step planimetric semiautomated segmentation as previously described.¹² The subsegmentation of WMH into SC and PV was made based on the discontinuity of the SC WMH, which are not touching the periventricular WMH, as compared to the PV WMH, which are in direct contact with the ventricles. WMH in contact with the ventricles that could be followed on 2 slices above the ventricles were considered as PV WMH. Above this level, WMH were considered as SC. Patients with severe confluent WMH were not subsegmented because there was no clear-cut distinction between PV and SC WMH. These cases were excluded from the relevant multivariable models exploring predictors for PV and SC WMH.

We defined and visually assessed 4 different subcortical WMH patterns on FLAIR MRI (figure 1), which emerged after evaluating WMH on hundreds of MRI scans from ICH patients over the years. The patterns included (1) multiple subcortical spots pattern—this pattern appears in SC white matter and it refers to small circles or spots of WMH (the total number of spots must be higher than 10 to meet this pattern requirement; this cutoff, though arbitrary, was prespecified based on its possible clinical usefulness as an easily identified pattern); (2) peri-BG pattern—WMH following the peripheral outline of the BG; (3) large (i.e., generally extending more than 5 mm in the deep white matter) posterior subcortical patches—large WMH volumes posterior to the ventricular horn with a visible separation between ventricle (with or without PV WMH); and (4) large (i.e., generally extending more than 5 mm in the deep white matter) anterior subcortical patches pattern—large WMH volumes anterior to the frontal horn/ventricle body junction with a clear distinction from PV WMH. The presence/absence of these 4 different subcortical WMH patterns was recorded irrespective of ICH presence; patterns were not mutually exclusive. Comparison between 2 trained raters (trained by reviewing a range of test cases based on the definitions and through discussion) using a sample of 20 cases reflecting the spectrum of WMH patterns presence and severity, and blinded to blood-sensitive MRI sequences and clinical data, showed excellent interrater agreement: kappa was 0.89 for

Figure 1 Different subcortical white matter hyperintensity (WMH) patterns on fluid-attenuated inversion recovery MRI



(A) Multiple subcortical spots WMH pattern. (B) Peri-basal ganglia WMH pattern. (C) Large posterior subcortical patches WMH pattern. (D) Anterior subcortical patches WMH pattern.

multiple spots pattern, 0.86 for peri-BG pattern, 0.82 for large anterior subcortical patches pattern, and 0.70 for large posterior subcortical patches.

Presence and number of CMBs and macrobleeds were evaluated on axial blood-sensitive MRI according to current consensus criteria.^{6,21} For purposes of statistical analyses, the number of lobar and deep CMBs was categorized using cutpoints as defined previously (0, 1, 2–4, or ≥ 5).²²

EPVS were assessed in line with STRIVE recommendations¹⁵; they were rated on axial T2-weighted MRI, in the BG and centrum semiovale (CSO), using a validated 4-point visual rating scale (0 = no PVS, 1 = <10 PVS, 2 = 11–20 PVS, 3 = 21–40 PVS, and 4 = >40 PVS).^{23–25} The assessment of EPVS was done blinded to CMB status and WMH patterns. We prespecified a dichotomized classification of EPVS degree as high (score >2) or low (score ≤ 2) in line with previous studies.^{8,25,26}

All MRI analyses were performed and recorded blinded to clinical and genetic information.

Statistics. Clinical, neuroimaging, and *APOE* characteristics of CAA-ICH vs HA-related ICH were compared in univariate analyses, using 2-sample *t* test, Wilcoxon rank sum, Pearson χ^2 , and Fisher exact tests as appropriate. Multivariable logistic regression analyses were performed to look for independent associations for each of the WMH patterns, including age, total WMH volume, lobar CMBs categories, deep CMBs categories, high CSO-EPVS grade, high BG-EPVS grade, as well as other biologically plausible covariates (e.g., hypertension). Stepwise forward variable selection ($p > 0.05$) was subsequently used to generate a minimal adjusted model. *APOE* genotype was analyzed as a categorical variable according to the presence or absence of

the $\epsilon 2$ or $\epsilon 4$ alleles. Separate logistic regression models were used to assess the relationship between *APOE* $\epsilon 2$ or $\epsilon 4$ allele presence and different WMH patterns.

All tests of significance were 2-tailed. Significance level was set at 0.05 for all analyses. Stata software (version 11.2; StataCorp, College Station, TX) was used for all analyses. The manuscript was prepared with reference to Strengthening the Reporting of Observational Studies In Epidemiology guidelines.²⁷

RESULTS Our final cohort included 319 CAA-ICH patients (6 pathology-definite, 18 probable with supportive pathology, 173 probable, and 122 true possible CAA [i.e., lobar ICH and no CMBs on MRI] according to the Boston criteria¹⁹) and 137 HA-ICH. The patients were enrolled between January 2003 and February 2012. Demographic, genetic, and imaging characteristics of the study population are presented in table 1. CAA patients were older (mean age 74 vs 67, $p < 0.001$) with a higher WMH burden (median total, PV, and SC WMH) on univariate analyses than HA-ICH cases (table 1). After correction for age, the total, PV, and SC WMH volumes were not different between the 2 groups. Older age and higher lobar and deep CMB counts were independent predictors of the total WMH volume ($p < 0.01$ for all predictors) after adjustment for sex and diagnosis (CAA vs HA) in a linear regression model (data not shown).

The prevalence of WMH patterns in the whole ICH cohort and according to diagnostic category is summarized in figure 2. In general, 198 (43.4%) of the ICH cases had at least one of these WMH patterns on MRI: 141 (30.9%) had only 1 of the 4 patterns, whereas 57 (12.5%) ICH cases had more than 1. The prevalence of multiple subcortical spots was higher in the CAA compared to the HA group (29.8% vs 16.8%; $p = 0.004$). In contrast, the peri-BG WMH pattern was more common in the HA- vs the CAA-ICH group (19% vs 7.8%; $p = 0.001$). In the cohort subset with genetic data available ($n = 271$), presence of *APOE* $\epsilon 2$ allele (but not $\epsilon 4$) showed a tendency for higher prevalence in patients with multiple subcortical spots compared to those without (25% vs 15.8%; $p = 0.075$). Adjustment for age and sex (odds ratio [OR] 1.75; 95% confidence interval [CI] 0.92–3.31, $p = 0.088$) did not alter the direction or strength of this association. None of the other WMH patterns showed an association with either *APOE* $\epsilon 2$ or $\epsilon 4$ presence.

In multivariable logistic regression analysis, the presence of multiple subcortical spots was independently associated with lobar CMBs (OR 1.23; 95% CI 1.01–1.50, $p = 0.039$) and high degree of CSO-EPVS (OR 2.43; 95% CI 1.56–3.80, $p < 0.0001$), after adjusting for age, hypertension, deep CMBs, total WMH volume, and high BG-EPVS degree (table 2). In a similar multivariable logistic

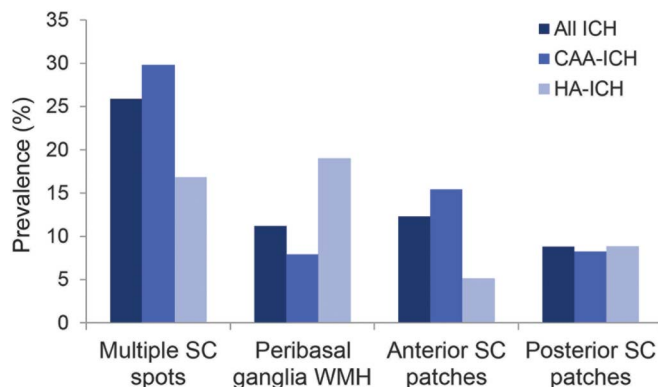
Table 1 Comparison of demographic, genetic, and neuroimaging (including WMH volumes and patterns) characteristics between CAA-ICH and HA-ICH patients

	CAA-ICH (n = 319)	HA-ICH (n = 137)	p Value
Age, y, mean (95% CI)	73.9 (72.7–75.1)	67.2 (64.8–69.5)	<0.001
Female, n (%)	161 (50.5)	59 (43.1)	0.147
Hypertension, n (%)	211 (66.1)	115 (83.9)	<0.0001
Diabetes, n (%)	44 (13.8)	35 (25.6)	0.002
Hypercholesterolemia, n (%)	139 (43.9)	55 (40.4)	0.502
History of ICH, n (%)	38 (11.9)	9 (6.6)	0.085
Any APOE ε2, n (%) ^a	39 (20)	12 (15.2)	0.373
Any APOE ε4, n (%) ^a	75 (38)	20 (21.1)	0.044
Lobar CMB count, median (IQR)	1 (0–3)	0	<0.001
Deep CMB count, median (range)	0	0 (0–14)	<0.001
Total WMH, mL, median (IQR)	19.7 (10.6–37)	12 (6.1–29.3)	<0.001
PV WMH, mL, median (IQR)	14.8 (8.8–28.2)	10.7 (5.7–22.1)	<0.001
SC WMH, mL, median (IQR)	2.3 (0.7–7.2)	1.6 (0.4–1.6)	0.029
Multiple SC spots, n (%)	95 (29.8)	23 (16.8)	0.004
Peri-BG WMH, n (%)	25 (7.8)	26 (19)	0.001
Anterior SC patches, n (%)	49 (15.4)	7 (5.1)	0.002
Posterior SC patches, n (%)	28 (8.2)	12 (8.8)	0.995
High degree of CSO-EPVS (>20), n (%)	138 (43.8)	24 (17.5)	<0.001
High degree of BG-EPVS (>20), n (%)	12 (3.8)	16 (11.7)	0.001

Abbreviations: BG = basal ganglia; CAA = cerebral amyloid angiopathy; CI = confidence interval; CMB = cerebral microbleeds; CSO = centrum semiovale; EPVS = enlarged perivascular spaces; HA = hypertensive arteriopathy; ICH = intracerebral hemorrhage; IQR = interquartile range; PV = periventricular; SC = subcortical; WMH = white matter hyperintensities.

^aAPOE genotype was available in 197 CAA patients and 79 HA cases.

Figure 2 Prevalence of white matter hyperintensity (WMH) patterns in the whole intracerebral hemorrhage (ICH) cohort and according to diagnostic category



Visual representation of the prevalence of WMH patterns observed in all ICH, cerebral amyloid angiopathy (CAA)-ICH, and hypertensive arteriopathy (HA)-ICH groups. For statistical comparisons, see table 1. SC = subcortical.

regression model, independent predictors associated with peri-BG WMH pattern were older age (OR 1.05; 95% CI 1.02–1.09, $p = 0.002$), deep CMBs (OR 2.46; 95% CI 1.44–4.20, $p = 0.001$), total WMH volume (OR 1.02; 95% CI 1.01–1.04, $p = 0.002$), and high degree of BG-EPVS (OR 8.81; 95% CI 3.37–23.02, $p < 0.0001$) (table 2). In the patient group with CAA-ICH, the presence of multiple subcortical spots was associated with higher lobar CMB counts (median 1, interquartile range 0–6 vs median 0, interquartile range 0–2, $p = 0.0032$ in CAA patients with vs without multiple subcortical spots, respectively). All models remained consistent and of similar effect size in sensitivity analyses excluding possible CAA cases ($n = 122$) or non-CAA-ICH cases without hypertension ($n = 22$).

The large posterior subcortical patches pattern was not independently related to any clinical or imaging predictors or CAA-ICH or HTN-ICH diagnoses. Large anterior subcortical patches were associated with total WMH volume (OR 1.03; 95% CI 1.02–1.05; $p < 0.0001$) and marginally with lobar CMBs (OR 1.27; 95% CI 0.98–1.63; $p = 0.07$), after adjusting for age, deep CMBs, and high CSO-EPVS and BG-EPVS degree in multivariable logistic regression.

DISCUSSION Our study in consecutive spontaneous ICH patients shows that WMH often appear in particular spatial patterns that can be reliably recognized on conventional MRI and that can associate with particular SVD or other putative MRI markers. The main findings are that CAA and HA relate to different patterns of subcortical WMH, despite both arteriopathies being associated with high total WMH burden. Multiple punctate subcortical FLAIR hyperintensities (i.e., multiple spots) are more commonly found in CAA and associated with lobar CMBs and high CSO-EPVS degree. This pattern may be an additional marker of cerebrovascular amyloid load or CAA-related leukoariosis. The lack of any association between age and the presence of multiple spots suggests that this pattern does not depend on age, increasing the chances to be used as a possibly early marker of CAA. Peri-BG WMH were more common in HA and linked to older age, higher WMH burden, deep CMBs, and high BG-EPVS degree.

Both CAA and HA are important contributors to microangiopathic subcortical injury leading to WMH.^{1,11,13,28} Based on the distinct topography of CAA and HA in the brain, one would expect striking differences in the regional distribution of WMH (similar to lobar vs deep CMBs) between these SVDs.¹³ Surprisingly, some studies suggest no major differences in overall WMH topography in CAA

Table 2 Multivariable logistic regression analyses of associations with multiple subcortical punctate hyperintense spots and peri-BG WMH patterns

	Multiple spots pattern		Peri-BG WMH	
	OR (95% CI)	p Value	OR (95% CI)	p Value
Age, y	1.01 (0.99-1.03)	0.391	1.06 (1.02-1.09)	0.002
Hypertension, yes vs no	1.01 (0.62-1.64)	0.961	1.00 (0.45-2.24)	0.996
Lobar CMB categories	1.23 (1.01-1.50)	0.039	0.75 (0.53-1.06)	0.105
Deep CMB categories	0.66 (0.34-1.28)	0.218	2.46 (1.44-4.20)	0.001
Total WMH, mL	1.00 (0.99-1.02)	0.416	1.02 (1.01-1.04)	0.002
High degree of CSO-EPVS (>20)	2.43 (1.56-3.80)	<0.0001	0.56 (0.25-1.25)	0.154
High degree of BG-EPVS (>20)	0.64 (0.22-1.87)	0.418	8.81 (3.37-23.02)	<0.0001

Abbreviations: BG = basal ganglia; CI = confidence interval; CMB = cerebral microbleeds; CSO = centrum semiovale; EPVS = enlarged perivascular spaces; OR = odds ratio; WMH = white matter hyperintensities.

compared to HA.^{7,14} The greatest lesion burden is in periventricular areas, typically around the frontal and occipital horns, indicating that white matter injury might occur through chronic microvascular ischemia in the most vulnerable regions.¹³ Studies that rely on voxel-based morphometry (VBM) suggest a relatively conserved anatomic distribution despite topographic differences across SVDs. Of note, the novel volumetric quantification of periventricular and subcortical WMH applied in the current large study cohort did not show any differences between CAA and HA. Therefore, classical VBM-based and volumetric methods are relatively insensitive to detect differences in WMH distribution across different SVDs and other innovative approaches are necessary to identify relatively specific patterns. A recent study that used quantitative methods has suggested a relative posterior distribution of WMH in CAA,²⁹ findings not surprising given the predilection of vascular amyloid pathology for posterior cortical regions.^{29,30} However, the quantitative methods used in this study were not geared toward providing practical tools to detect such a gradient in a nonresearch setting. The WMH patterns described in our study are easy to identify using clinical MRI as evidenced by high interrater agreements but our study also showed that developing a subcortical WMH rating system that has high sensitivity/specificity to diagnose the underlying SVD is a difficult undertaking, a conclusion similar to previous reports.^{29,31}

The rather significant overlap of the WMH patterns in patients with CAA- and HTN-ICH suggest that leukoaraiosis is probably multifactorial in most cases. The predominant contributions of CAA and HA might nevertheless be identified in at least some individuals. Our results indeed provide an alternative simple strategy for utilizing different WMH patterns

as additional markers of the dominant microvasculopathy type in older individuals with ICH and require further clinical attention. The multiple subcortical spots pattern seems to be more associated with CAA, a finding supported by its strong relation with established imaging markers of the disease, including lobar CMBs. Second, this association being independent of the total WMH burden in multivariable analysis may imply different pathophysiologic mechanisms, perhaps related to more focal effects of superficial cortical amyloid-laden vessels. The peri-BG WMH pattern correlates well with the underlying anatomical distribution and burden of HA in the small deep perforators. However, we found that it is also strongly related to the total WMH lesion volume, and might partly reflect a more advanced stage in the pathophysiology of WMH in general.

Emerging data show that the topography of EPVS differs according to the underlying SVD: CSO-EPVS with CAA and BG-EPVS with HA.^{8,9,25} It is thus not surprising that high CSO-EPVS burden (but not BG-EPVS) is independently related to multiple spots, while high BG-EPVS degree (but not CSO-EPVS) is linked to the peri-BG WMH pattern in our study population. In addition, these lesions tended to cluster together (i.e., CSO-EPVS/multiple WMH spots pattern; BG-EPVS/peri-BG WMH pattern) as markers of the same small vessel pathologies; they therefore might be pathophysiologically linked to each other.

Notable strengths of our study include the systematic evaluation of MRI scans by trained raters using validated scales for a comprehensive range of imaging markers of SVD, the volumetric assessment of total WMH volume, and the use of prespecified WMH patterns. The large sample size of consecutive ICH patients in our cohort allowed us to build robust multivariable models. A limitation is the potential selection bias due to the requirement for MRI done as part of clinical care and the lack of *APOE* data in around 40% of patients. Our cohort had more CAA-ICH than HA-ICH patients, a known issue in all previous studies in the field; still, our study included a high number of HA-ICH when compared to previous work.³² Another limitation is the relative uncertainty of categorization of the underlying arteriopathy in the absence of pathologic data, despite our best efforts to have well-defined groups, including purely lobar CAA-related bleeds vs purely deep bleeds, presumably related to non-CAA HA process. Such diagnostic uncertainty would only favor null hypothesis but we have been able to demonstrate significant associations between 2 imaging markers and SVDs. These drawbacks exist for all large-scale studies that analyze data from ICH cohorts without pathologic confirmation.

Our work shows that different patterns of subcortical white matter damage can provide insights on the dominant type of underlying arteriopathy as well as potential mechanisms: multiple punctate FLAIR hyperintensities (i.e., spots) correlate with CAA and CAA-related imaging markers, while peri-BG WMH pattern is strongly linked to HA and HA-related markers. Our findings will need to be studied further in different cohorts and especially their significance in detecting the predominant SVD type in early (presymptomatic) phases as well as predicting disease course would need to be explored.

AUTHOR CONTRIBUTIONS

Statistical analysis was conducted by Dr. A. Charidimou and Dr. M.E. Gurol. A. Charidimou: project design, imaging analysis, data analysis, writeup. G. Boulouis: project design, imaging analysis, critical revisions. K. Haley: imaging analysis, critical revisions. E. Auriel: imaging analysis, critical revisions. E.S. van Etten: imaging analysis, critical revisions. P. Fotiadis: critical revisions. Y. Reijmer: critical revisions. A. Ayres: data collection and management. A. Vashkevich: data collection and management. Z.Y. Dipucchio: data collection and management. K.M. Schwab: data collection and management. S. Martinez-Ramirez: imaging analysis, critical revisions. S.M. Greenberg: funding, data collection, critical revisions. M.E. Gurol: project concept and design, data collection, data analysis, writeup, critical revisions.

STUDY FUNDING

Supported by the following NIH grants: 5K23NS083711 (M.E.G.), R01 NS070834, and 2R01 AG26484 (S.M.G.).

DISCLOSURE

The authors report no disclosures relevant to the manuscript. Go to Neurology.org for full disclosures.

Received July 31, 2015. Accepted in final form October 12, 2015.

REFERENCES

- Pantoni L. Cerebral small vessel disease: from pathogenesis and clinical characteristics to therapeutic challenges. *Lancet Neurol* 2010;9:689–701.
- Charidimou A, Gang Q, Werring DJ. Sporadic cerebral amyloid angiopathy revisited: recent insights into pathophysiology and clinical spectrum. *J Neurol Neurosurg Psychiatry* 2012;83:124–137.
- Viswanathan A, Greenberg SM. Cerebral amyloid angiopathy in the elderly. *Ann Neurol* 2011;70:871–880.
- Arvanitakis Z, Leurgans SE, Wang Z, Wilson RS, Bennett DA, Schneider JA. Cerebral amyloid angiopathy pathology and cognitive domains in older persons. *Ann Neurol* 2011;69:320–327.
- Greenberg SM, Salman RA, Biessels GJ, et al. Outcome markers for clinical trials in cerebral amyloid angiopathy. *Lancet Neurol* 2014;13:419–428.
- Greenberg SM, Vernooij MW, Cordonnier C, et al. Cerebral microbleeds: a guide to detection and interpretation. *Lancet Neurol* 2009;8:165–174.
- Smith EE, Nandigam KR, Chen YW, et al. MRI markers of small vessel disease in lobar and deep hemispheric intracerebral hemorrhage. *Stroke* 2010;41:1933–1938.
- Martinez-Ramirez S, Pontes-Neto OM, Dumas AP, et al. Topography of dilated perivascular spaces in subjects from a memory clinic cohort. *Neurology* 2013;80:1551–1556.

- Charidimou A, Meegahage R, Fox Z, et al. Enlarged perivascular spaces as a marker of underlying arteriopathy in intracerebral haemorrhage: a multicentre MRI cohort study. *J Neurol Neurosurg Psychiatry* 2013;84:624–629.
- Dumas A, Dierksen GA, Gurol ME, et al. Functional magnetic resonance imaging detection of vascular reactivity in cerebral amyloid angiopathy. *Ann Neurol* 2012;72:76–81.
- Gurol ME, Viswanathan A, Gidicsin C, et al. Cerebral amyloid angiopathy burden associated with leukoaraiosis: a positron emission tomography/magnetic resonance imaging study. *Ann Neurol* 2013;73:529–536.
- Gurol ME, Irizarry MC, Smith EE, et al. Plasma beta-amyloid and white matter lesions in AD, MCI, and cerebral amyloid angiopathy. *Neurology* 2006;66:23–29.
- Smith EE. Leukoaraiosis and stroke. *Stroke* 2010;41: S139–S143.
- Holland CM, Smith EE, Csapo I, et al. Spatial distribution of white-matter hyperintensities in Alzheimer disease, cerebral amyloid angiopathy, and healthy aging. *Stroke* 2008;39:1127–1133.
- Wardlaw JM, Smith EE, Biessels GJ, et al. Neuroimaging standards for research into small vessel disease and its contribution to ageing and neurodegeneration. *Lancet Neurol* 2013;12:822–838.
- Auriel E, Gurol ME, Ayres A, et al. Characteristic distributions of intracerebral hemorrhage-associated diffusion-weighted lesions. *Neurology* 2012;79:2335–2341.
- O'Donnell HC, Rosand J, Knudsen KA, et al. Apolipoprotein E genotype and the risk of recurrent lobar intracerebral hemorrhage. *N Engl J Med* 2000;342:240–245.
- van Etten ES, Auriel E, Haley KE, et al. Incidence of symptomatic hemorrhage in patients with lobar microbleeds. *Stroke* 2014;45:2280–2285.
- Knudsen KA, Rosand J, Karluk D, Greenberg SM. Clinical diagnosis of cerebral amyloid angiopathy: validation of the Boston criteria. *Neurology* 2001;56:537–539.
- Brouwers HB, Biffi A, McNamara KA, et al. Apolipoprotein E genotype is associated with CT angiography spot sign in lobar intracerebral hemorrhage. *Stroke* 2012;43: 2120–2125.
- Kidwell CS, Greenberg SM. Red meets white: do microbleeds link hemorrhagic and ischemic cerebrovascular disease? *Neurology* 2009;73:1614–1615.
- Biffi A, Halpin A, Towfighi A, et al. Aspirin and recurrent intracerebral hemorrhage in cerebral amyloid angiopathy. *Neurology* 2010;75:693–698.
- Doubal FN, MacLulich AM, Ferguson KJ, Dennis MS, Wardlaw JM. Enlarged perivascular spaces on MRI are a feature of cerebral small vessel disease. *Stroke* 2010;41: 450–454.
- MacLulich AM, Wardlaw JM, Ferguson KJ, Starr JM, Seckl JR, Deary IJ. Enlarged perivascular spaces are associated with cognitive function in healthy elderly men. *J Neurol Neurosurg Psychiatry* 2004;75:1519–1523.
- Charidimou A, Jaunmuktane Z, Baron JC, et al. White matter perivascular spaces: an MRI marker in pathology-proven cerebral amyloid angiopathy? *Neurology* 2014;82:57–62.
- Zhu YC, Tzourio C, Soumare A, Mazoyer B, Dufouil C, Chabriat H. Severity of dilated Virchow-Robin spaces is associated with age, blood pressure, and MRI markers of small vessel disease: a population-based study. *Stroke* 2010;41:2483–2490.
- von Elm E, Altman DG, Egger M, Pocock SJ, Gotsche PC, Vandenbroucke JP. The Strengthening the

- Reporting of Observational Studies in Epidemiology (STROBE) statement: guidelines for reporting observational studies. *Lancet* 2007;370:1453–1457.
28. Reijmer YD, Fotiadis P, Martinez-Ramirez S, et al. Structural network alterations and neurological dysfunction in cerebral amyloid angiopathy. *Brain* 2015;138:179–188.
 29. Thanprasertsuk S, Martinez-Ramirez S, Pontes-Neto OM, et al. Posterior white matter disease distribution as a predictor of amyloid angiopathy. *Neurology* 2014;83:794–800.
 30. Vinters HV, Gilbert JJ. Cerebral amyloid angiopathy: incidence and complications in the aging brain: II: the distribution of amyloid vascular changes. *Stroke* 1983; 14:924–928.
 31. Zhu YC, Chabriat H, Godin O, et al. Distribution of white matter hyperintensity in cerebral hemorrhage and healthy aging. *J Neurol* 2012;259:530–536.
 32. Charidimou A, Jager RH, Fox Z, et al. Prevalence and mechanisms of cortical superficial siderosis in cerebral amyloid angiopathy. *Neurology* 2013;81:626–632.

Experience the Excellence of the 2016 AAN Annual Meeting

Registration is now open for the 68th AAN Annual Meeting, set to take place Friday, April 15, through Thursday, April 21, 2016, at the Vancouver Convention Centre in Vancouver, BC, Canada. Experience the excellence of new, exciting changes, including: one low, single registration rate; more than 230 education programs in two-hour increments; plenary sessions every day starting Friday; scientific poster sessions every day starting Saturday; interactive and experiential learning and networking opportunities all week long, and more! The money-saving early registration deadline is March 24, 2016. Visit AAN.com/view/AM16 and register today!

Visit the *Neurology*[®] Web Site at Neurology.org

- Enhanced navigation format
- Increased search capability
- Highlighted articles
- Detailed podcast descriptions
- RSS Feeds of current issue and podcasts
- Personal folders for articles and searches
- Mobile device download link
- AAN Web page links
- Links to *Neurology Now*[®], *Neurology Today*[®], and *Continuum*[®]
- Resident & Fellow subsite

 Find *Neurology*[®] on Facebook: <http://tinyurl.com/neurologyfan>

 Follow *Neurology*[®] on Twitter: <https://twitter.com/GreenJournal>